



RESEARCH LETTER

10.1002/2016GL069786

Key Points:

- Assumed particle morphology affects the retrieval of light-absorbing organic aerosol absorptivity
- Assumed morphology affects the direct radiative effect calculations in large-scale models
- Consistency in the assumed morphology between retrievals and models is key

Supporting Information:

- Supporting Information S1

Correspondence to:

R. Saleh,
rawad@uga.edu

Citation:

Saleh, R., P. J. Adams, N. M. Donahue, and A. L. Robinson (2016), The interplay between assumed morphology and the direct radiative effect of light-absorbing organic aerosol, *Geophys. Res. Lett.*, *43*, 8735–8743, doi:10.1002/2016GL069786.

Received 27 MAY 2016

Accepted 19 JUL 2016

Accepted article online 22 JUL 2016

Published online 24 AUG 2016

The interplay between assumed morphology and the direct radiative effect of light-absorbing organic aerosol

Rawad Saleh^{1,2}, Peter J. Adams¹, Neil M. Donahue¹, and Allen L. Robinson¹

¹Center for Atmospheric Particle Studies, Carnegie Mellon University, Pittsburgh, Pennsylvania, USA, ²Now at College of Engineering, University of Georgia, Athens, Georgia, USA

Abstract Mie theory is widely employed in aerosol top-of-the-atmosphere direct radiative effect (DRE) calculations and to retrieve the absorptivity of light-absorbing organic aerosol (OA) from measurements. However, when OA is internally mixed with black carbon, it may exhibit complex morphologies whose optical behavior is imperfectly predicted by Mie theory, introducing bias in the retrieved absorptivities. We performed numerical experiments and global radiative transfer modeling (RTM) to investigate the effect of this bias on the calculated absorption and thus the DRE. We show that using true OA absorptivity, retrieved with a realistic representation of the complex morphology, leads to significant errors in DRE when the RTM employs the simplified Mie theory. On the other hand, when Mie theory is consistently applied in both OA absorptivity retrieval and the RTM, the errors largely cancel out, yielding accurate DRE. As long as global RTMs use Mie theory, they should implement parametrizations of light-absorbing OA derived from retrievals based on Mie theory.

1. Introduction

Light absorption by organic aerosol (OA) due to the presence of brown carbon (BrC) [Andreae and Gelencser, 2006] has been shown to be an important contributor to the global aerosol direct radiative effect (DRE) [Jacobson, 2012, 2014; Feng et al., 2013; Lin et al., 2014; Wang et al., 2014; Kordos et al., 2015; Saleh et al., 2015]. However, there are major uncertainties compromising the accuracy of estimates of the climate effect of light-absorbing OA. Two important sources of this uncertainty stem from the difficulties associated with (1) retrieving OA absorptivity (imaginary part of the refractive index) from measurements and (2) constraining the morphology of OA-containing particles and the extent of the associated absorption enhancement by lensing due to OA coating over black carbon (BC) cores [Schnaiter, 2005; Bond et al., 2006; Zhang et al., 2008; Adachi et al., 2010; Lack and Cappa, 2010; Cappa et al., 2012; Saleh et al., 2013, 2014]. Crucially, these two sources of uncertainty are interdependent. This interdependence, which is the focus of this paper, is manifested both in the retrieval of optical properties from measurements [D. Liu et al., 2015] as well as in global radiative transfer calculations [Saleh et al., 2015].

Measurement of the absorptivity of light-absorbing OA is challenging mainly because it is usually coemitted with BC. One must decouple the absorption by these two components in order to isolate the optical properties of each. Two approaches are commonly employed to achieve this. One approach relies on physically separating OA from BC by extracting the OA from filter samples using a solvent (e.g., water or methanol) and measuring the OA absorptivity in the resulting solution [Kirchstetter et al., 2004; Adler et al., 2010; Chen and Bond, 2010; Di Lorenzo and Young, 2016]. While this method provides accurate absorptivity measurements of the extracts, the drawbacks are low time resolution and the potential for bias because a significant fraction of BrC might be either nonextractable or chemically altered by solvents. In the second approach, OA absorptivity is retrieved by fitting an absorption model to real-time absorption measurements [Lack et al., 2012; Saleh et al., 2013, 2014]. This method has high time resolution and avoids chemical extraction. However, absorption calculations require knowledge of the morphology, which is usually poorly constrained. This can introduce large uncertainties. D. Liu et al. [2015] investigated the effect of assumed particle morphology on the retrieved absorptivity of light-absorbing OA emitted by wood burning in London. They treated the carbonaceous particles as either spherical with a core (BC)-shell (OA) morphology, which they modeled using Mie theory [Bohren and Huffman, 1983] or aggregates of BC spherules coated with OA, which they modeled using Rayleigh-Debye-Gans (RDG) approximation [Sorensen, 2001; Moosmüller and Arnott, 2009]. The retrieved absorptivities varied by a factor of 4 depending on the assumed morphology.

The interplay between morphology and OA absorption also affects atmospheric radiative transfer calculations. *Saleh et al.* [2015] calculated the global DRE of carbonaceous biomass-burning aerosol with two mixing state/morphology assumptions—either internally mixed with core-shell morphology or externally mixed. In terms of optical behavior, the internally mixed core-shell case exhibits absorption enhancement by lensing, while the externally mixed case is similar to an internally mixed case with the BC residing on the edge of OA particles, thus exhibiting negligible lensing [Adachi et al., 2010; Cappa et al., 2012]. Due to the lensing effect, the mean global DRE increased by $+0.29 \text{ W/m}^2$ for the core-shell case over the externally mixed case; however, the contribution of OA absorption dropped from $+0.22 \text{ W/m}^2$ to $+0.12 \text{ W/m}^2$. The reason for this—perhaps counterintuitive—result is that an absorbing OA coating diminishes the intensity of light refracted into the BC core [Lack and Cappa, 2010], thus reducing the lensing effect (see Figure 4 and discussion in *Saleh et al.* [2015]). Consequently, a portion of the OA absorption is offset by the decrease in lensing, causing the overall effect of OA absorption to be smaller in the core-shell case relative to the externally mixed case.

While large-scale radiative transfer models (RTMs) mostly assume spherical carbonaceous particles and use Mie theory to calculate their optical properties, the true morphology of BC-containing particles in the atmosphere is widely debated. There is growing evidence that BC-containing particles can exhibit complex morphologies [e.g., Fu et al., 2012; China et al., 2013; Zhu et al., 2013; Chakrabarty et al., 2014; Giordano et al., 2015], which are imperfectly represented using Mie theory [Adachi et al., 2010; Cappa et al., 2012]. Consequently, a growing body of literature has focused on constraining these morphologies and developing appropriate mathematical models to represent their absorption [Adachi et al., 2010; Yurkin and Hoekstra, 2011; Mishchenko et al., 2013; Wu et al., 2016].

To summarize, (1) light-absorbing OA plays an important role in governing the aerosol climate effect; (2) the morphology of carbonaceous particles is both complex and variable; and (3) both global DRE estimates and retrievals of light-absorbing OA absorptivities are sensitive to the assumed morphology. It is expected that new studies will focus on retrieving absorptivities of atmospheric light-absorbing OA and that these studies will strive to account for the complex particle morphology in their analysis. These endeavors will require the application of sophisticated imaging techniques (e.g., electron microscopy) and optical modeling (e.g., discrete dipole approximation). One objective of these studies will be to provide these OA optical properties to modelers for use in RTMs.

Although it is possible that these studies will succeed in their complex task, embedding such sophisticated treatments in large-scale RTMs might be prohibitively expensive. It requires tracking the spatial and temporal diversity of particle morphologies and performing the associated complex optical calculations. Therefore, even though the treatment of the complex morphology of BC-containing particles may become common in studies retrieving OA absorptivities from measurements, it is highly likely that the simplified spherical assumption (Mie theory) will still be the model of choice in large-scale RTMs, at least for the near future.

In this paper, we investigate potential biases in calculated absorption, and thus DRE estimates, caused by this inconsistency in the treatment of morphology between OA absorptivity retrievals and RTM calculations. In the subsequent sections, we describe the results from a thought experiment, involving numerical measurements and RTM calculations. We focus on emissions from biomass burning, the largest global contributor of atmospheric carbonaceous aerosols [Bond et al., 2004].

2. The Thought Experiment

To investigate the effect of assumed particle morphology on the DRE of biomass-burning carbonaceous aerosols, we designed a thought experiment involving the following steps. First, we generated numerical pseudo “measurements” of absorption by carbonaceous (BC + OA) biomass-burning particles that simulated common measurements performed in the laboratory [e.g., Lambe et al., 2013; Saleh et al., 2013, 2014; Liu et al., 2014] or in the field [e.g., Cappa et al., 2012; Lack et al., 2012; D. Liu et al., 2015; S. Liu et al., 2015]. We then retrieved the absorptivity (imaginary part of the refractive indices; k_{OA}) of OA using two optical models: (1) a realistic model based on the “true” complex particle morphology and (2) a simplified model based on spherical core-shell morphology. We used the resulting $k_{\text{OA,true}}$ and $k_{\text{OA,simplified}}$ as inputs to a global RTM to calculate the DRE of biomass-burning carbonaceous aerosols. We performed three RTM simulations with (1) realistic treatment of the morphology and $k_{\text{OA,true}}$ (true and true), (2) simplified treatment of the

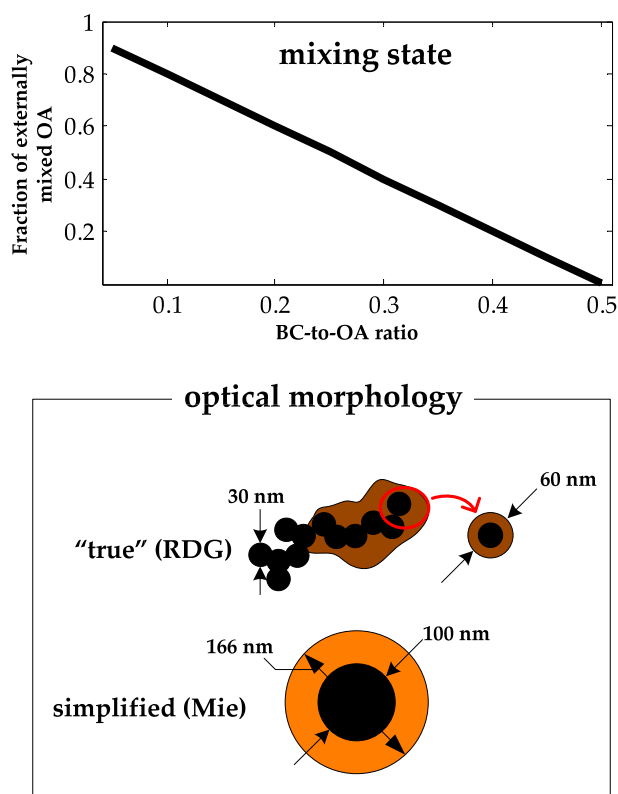


Figure 1. (top) BC and OA mixing state and (bottom) optical morphology assumed in the retrieval of OA imaginary part of the refractive indices and global radiative transfer calculations.

externally mixed particles) was consistent between the k_{OA} retrievals and the RTM. We parameterized the mixing state based on the expectation that it depends on the relative abundance of the two components. BC particles form inside the flame zone, and as the emissions cool, organic vapors become supersaturated and condense (form OA). The BC particles provide surface area onto which supersaturated vapors condense, forming internally mixed particles. A portion of the organics can also nucleate and form externally mixed particles. The relative abundance of externally and internally mixed OA depends on the condensation sink provided by BC particles and the energy barrier for nucleation. Since biomass-burning emissions have relatively high OA loadings, most of the BC is expected to be internally mixed with OA, while a fraction of the OA would be externally mixed [Schwarz *et al.*, 2008; Lack *et al.*, 2012; China *et al.*, 2013; Saleh *et al.*, 2013, 2014]. We parameterized the mixing state as a function of the mass BC-to-OA ratio as shown in Figure 1. The 0.05–0.5 bounds for the BC-to-OA ratio are representative of biomass-burning emissions [Saleh *et al.*, 2015]. To simplify the calculations, we assumed all OA to be internally mixed with BC at BC-to-OA ratio of 0.5. For smaller BC-to-OA ratios, we assumed that the excess OA formed externally mixed particles with a size of 150 nm. For the internally mixed particles, we calculated the OA coating thickness corresponding to a BC-to-OA ratio of 0.5 and assumed the same coating thickness for smaller BC-to-OA ratios (i.e., all the additional OA formed externally mixed particles).

We assumed that the morphology of biomass-burning particles featured BC aggregates engulfed in OA. We explored a range of BC monomer sizes (10 nm–50 nm) and fraction of BC monomers coated by OA (0.1–1) in the simplified RT calculations. In the global RTM, we focused on a single configuration (30 nm BC monomers with 50% coated by OA). From the perspective of k_{OA} retrieval and RTM calculations, the morphology of a particle affects its optical behavior. It is therefore useful to define “optical morphology” as the morphology assumed so that a certain optical model can be applied to represent the optical behavior of a particle having a complex morphology. As outlined in section 2, we considered two optical morphologies in the k_{OA} retrievals and RTM calculations (Figure 1):

morphology and $k_{OA,true}$ (simplified and true), and (3) simplified treatment of the morphology and $k_{OA,simplified}$ (simplified and simplified). The first case (true and true) yields the true DRE within the context of this thought experiment. We compared the DRE values obtained from the other two cases with this true case to assess parameterization biases.

Due to the high computational cost, we considered only a single complex morphology in the global RTM calculations. We explored the effect of a wide range of morphologies by performing simplified radiative transfer (RT) calculations.

3. Mixing State and Optical Morphology

The k_{OA} retrievals (from the pseudo measurements) and the RTM calculations outlined in section 2 both require representation of the mixing state and morphology of the biomass-burning particles.

Treatment of the mixing state of BC and OA (the fraction of internally versus

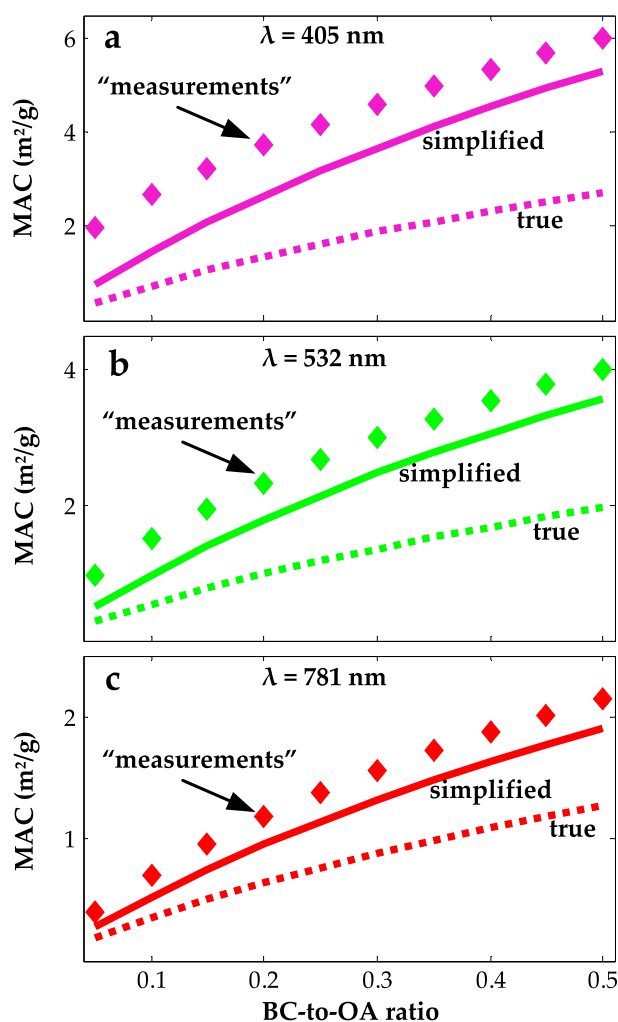


Figure 2. Results from the numerical experiments. Symbols are MAC values derived from numerical pseudo measurements that covered a range of BC-to-OA ratios (0.05–0.5) at (a) violet, (b) green, and (c) red wavelengths. Lines are calculated MAC values assuming nonabsorbing OA and either true (dotted) or simplified (solid) optical morphologies. The difference between the lines and symbols corresponds to the contribution of BrC to absorption. At all wavelengths, MAC calculated using the simplified optical morphology is larger than using the true morphology. Thus, performing optical closure with the true optical morphology would yield larger k_{OA} values than simplified optical morphology.

prised of 100 nm spherical BC cores with OA forming uniform spherical coatings around the BC cores. In the subsequent sections, this optical morphology, and the k_{OA} and DRE values obtained using this optical morphology, are labeled “simplified.”

4. Retrieval of OA Imaginary Part of the Refractive Indices

We retrieved biomass-burning k_{OA} values from numerical light absorption pseudo measurements using optical closure [Lack et al., 2012; Saleh et al., 2013, 2014; D. Liu et al., 2015]. We generated pseudo measurements of aerosol mass absorption cross sections (total absorption cross section per unit total aerosol mass; MAC (m²/g)) at three wavelengths of 405, 532, and 781 nm. We chose these wavelengths to simulate data obtained from the widely used photoacoustic soot spectrometer (PASS-3, DMT). We then fitted the

1. We assumed that the BC monomers forming the aggregates behaved as independent absorbers for which the RDG approximation [Sorensen, 2001; Moosmüller and Arnott, 2009] was valid. The OA coating was distributed equally across the engulfed monomers, which we treated as spherical core-shell [D. Liu et al., 2015]. We assumed that this optical morphology exactly predicted light absorption by the biomass-burning particles. This is justified because the purpose of our thought experiment is to investigate the effect of adopting a simplified optical morphology to represent absorption by particles with a complex morphology. The type of optical morphology representing the “true behavior” of the particles in this thought experiment is not important as long as the simplified and true optical morphologies exhibit a significant enough divergence in behavior to present a stringent test to the effect of inconsistency in assumed optical morphology. As will be shown in section 4 and section 5, using RDG as the true optical morphology fulfills this condition. Therefore, adopting the straightforward RDG model instead of a more computationally involved model is sensible. In the subsequent sections, this optical morphology, and the k_{OA} and DRE values obtained using this optical morphology, are labeled true.

2. We adopted the simplified core-shell Mie theory as the optical morphology. In this simplified treatment, the biomass-burning particles were com-

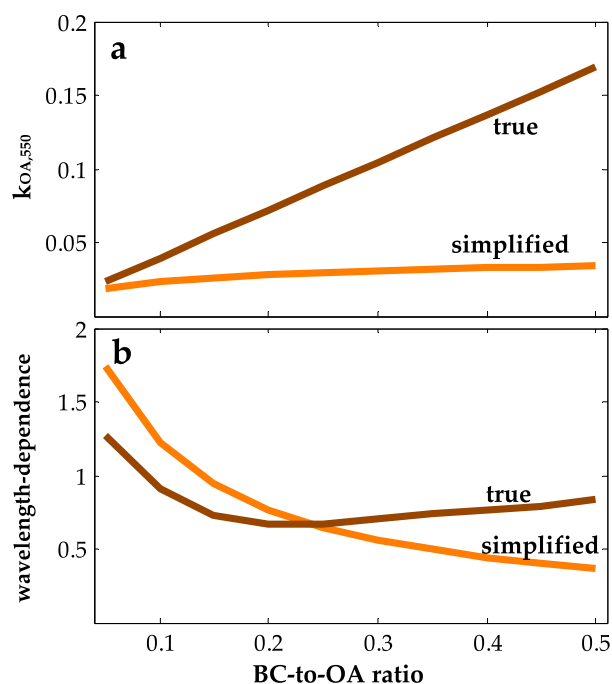


Figure 3. Imaginary part of the (a) refractive indices at 550 nm and their (b) wavelength dependence as a function of BC-to-OA ratio retrieved from the numerical experiments using true and simplified optical morphologies.

between model calculations and measurements. As evident in Figure 2, absorption by the BC portion of the particles (including absorption enhancement by lensing) is smaller for the true optical morphology than for the simplified optical morphology. Consequently, performing the retrieval using the true optical morphology results in a larger BrC effect (larger retrieved k_{OA} values). The retrieved k_{OA} as function of BC-to-OA ratio for the true ($k_{OA,true}$) and simplified ($k_{OA,simplified}$) optical morphologies is shown in Figure 3. Following Saleh *et al.* [2013], Figure 3a shows k_{OA} at wavelength (λ) of 550 nm ($k_{OA,550}$) and Figure 3b shows the wavelength dependence of k_{OA} (w ; where $k_{OA} = k_{OA,550} \times [550/\lambda]^w$). Saleh *et al.* [2014] showed that k_{OA} of biomass-burning emissions increases with increasing BC-to-OA ratio. We designed the thought experiment in this study such that the retrieved k_{OA} would exhibit a similar dependence on the BC-to-OA ratio. Furthermore, we generated the pseudo measurements by calculating MAC values assuming core-shell Mie theory and the k_{OA} values of Saleh *et al.* [2014]. In other words, we generated the pseudo measurement such that the simplified optical morphology would yield the same k_{OA} values as the parameterization of Saleh *et al.* [2014], which was developed using Mie theory (i.e., the simplified optical morphology). As expected from the model-measurement comparison in Figure 2, the k_{OA} values retrieved using the true optical morphology are larger than those retrieved using the simplified optical morphology. The deviation between the two increases with increasing BC-to-OA ratio, because the fraction of externally mixed OA decreases (Figure 1), adding more weight to the effect of the morphology of the internally mixed particles. We note that $k_{OA,true}$ is true only in the context of this thought experiment because the true optical morphology used to retrieve $k_{OA,true}$ is not necessarily an accurate representation of real-life biomass-burning particles. However, as we emphasized in section 3 and as Figure 3 clearly shows, there is significant difference between $k_{OA,simplified}$ and $k_{OA,true}$, thus presenting a stringent test to the effect of inconsistency in assumed optical morphology.

5. Radiative Transfer Modeling

The next step in the thought experiment was to perform global RTM simulations using the retrieved $k_{OA,true}$ and $k_{OA,simplified}$ values.

measurements using optical calculations, with k_{OA} as the free parameter. The optical calculations require the following inputs: BC refractive index (assumed to be $1.85 + 0.71i$) [Bond and Bergstrom, 2005]; OA real part of the refractive index (assumed to be 1.7) [Saleh *et al.*, 2014]; and, finally, the optical morphology and BC and OA mixing state, which we obtained as described in section 3.

Numerical pseudo measurements of MAC as a function of BC-to-OA ratio at the three wavelengths (405, 532, and 781 nm) are shown in Figure 2. Also shown are model calculations, assuming nonabsorbing OA (i.e., $k_{OA} = 0$), for both the true and simplified optical morphologies described in section 3. We show results only for one of the morphology cases (30 nm BC monomers with OA coating half of the monomers). The difference between the model calculations and the pseudo measurements is due to OA (BrC) absorption. The k_{OA} retrieval process involves optimizing for the k_{OA} values that yield the best agreement

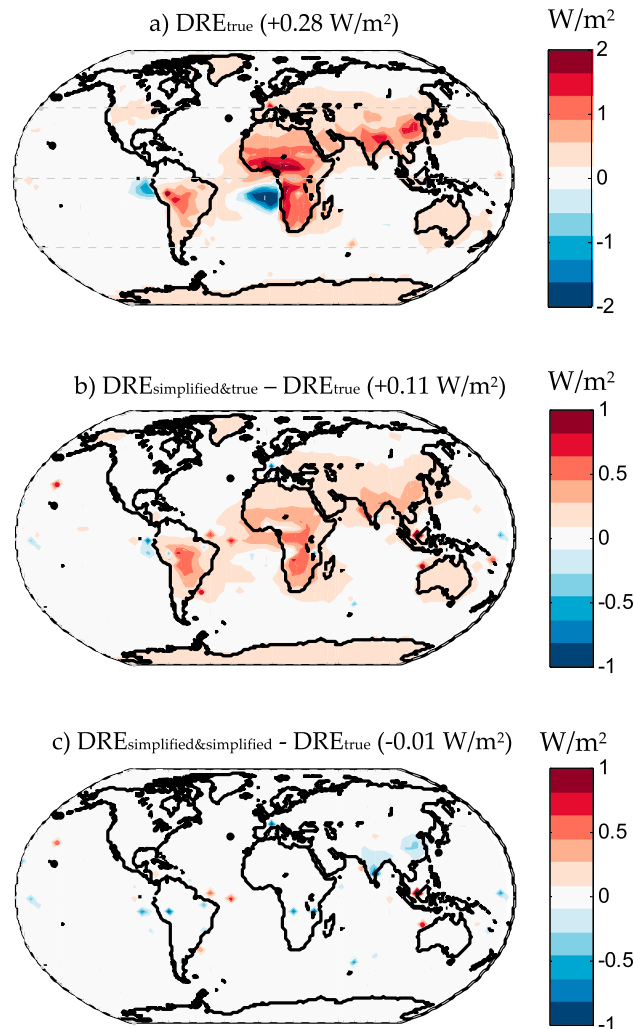


Figure 4. Effect of the optical morphology and OA imaginary part of the refractive indices (k_{OA}) on the global distribution of DRE of carbonaceous aerosols emitted by biomass burning. Numbers in parentheses are global averages. (a) The true DRE (DRE_{true}) calculated using the true optical morphology and true k_{OA} ($k_{OA,true}$; retrieved using the true optical morphology). (b) The difference between DRE calculated using the simplified optical morphology and $k_{OA,true}$ ($DRE_{simplified\&true}$) and DRE_{true} . (c) The difference between DRE calculated using the simplified optical morphology and $k_{OA,simplified}$ ($DRE_{simplified\&simplified}$) and DRE_{true} .

RTM calculations. These properties included the absorption coefficients (b_{abs} : total absorption cross section per unit volume of air), scattering coefficients (b_{sca} : total scattering cross section per unit volume of air), and asymmetry parameters (g , which represents the angular distribution of scattering). We calculated b_{abs} using the three cases described in section 2: (1) true optical morphology and $k_{OA,true}$ (true and true), (2) simplified optical morphology and $k_{OA,true}$ (simplified and true), and (3) simplified optical morphology and $k_{OA,simplified}$ (simplified and simplified). To isolate the effect of the interplay between morphology and OA absorption, which is the focus of this paper, we calculated b_{sca} and g using the simplified optical morphology for all cases. In these calculations, we applied the mixing state parameterization in Figure 1 to BC and OA from all sources, as well as inorganic sulfates and nitrates. In other words, we replaced the BC-to-OA ratio in Figure 1 with the BC-to-“non-BC” ratio.

We used the global fields of optical properties (b_{abs} , b_{sca} , and g) as input to the RTM libRadtran [Mayer and Kylling, 2005] to calculate the biomass-burning carbonaceous aerosol DRE for the three cases. libRadtran

The global RTM simulations followed the procedure of Saleh *et al.* [2015]; here we provide only a brief description. We simulated monthly averages, for the year 2005, of the global distribution of speciated aerosol concentrations (horizontal resolution of 4° latitude \times 5° longitude and 47 vertical layers) using v9-01-03 of the global chemical-transport model GEOS-Chem. To determine the concentration of carbonaceous aerosols emitted by biomass burning, we ran GEOS-Chem twice, once with and once without the biomass-burning emissions. We attributed the difference in BC and OA concentrations between the two simulations to biomass burning. The yearly mean of the global distribution of biomass-burning BC-to-OA ratios is shown in Figure S1. The water content of the aerosol particles was estimated using k-Köhler theory [Petters and Kreidenweis, 2007]. The Kappa parameter values for different components are given in Saleh *et al.* [2015]. We assumed that biomass-burning OA was well mixed with OA from other sources as well as with inorganic sulfates and nitrates, and we calculated the average refractive index of the mixture using the volume mixing rule. The refractive indices of the different components are given in Saleh *et al.* [2015].

We used monthly averages of the aerosol fields to calculate the aerosol optical properties needed for

solves the radiative transfer equation using the six-stream solver developed by Stamnes *et al.* [2000]. The column distributions of pressure, temperature, as well as densities of ozone, oxygen, water vapor, CO₂, and NO₂ were based on the spatial and temporal distributions specified by Anderson *et al.* [1986]. We obtained the cloud coverage from observations by NASA's International Satellite Cloud Climatology Project at a horizontal resolution of 2.5° × 2.5° and downgraded to the GEOS-Chem grid (4° × 5°). We accounted for cloud overlap using the maximum random overlap assumption.

We averaged monthly biomass-burning DRE values to obtain the yearly mean DRE (for the year 2005) depicted in Figure 4. Figure 4a shows DRE calculated with k_{OA} retrieved using the true optical morphology ($k_{\text{OA,true}}$), as well as using the true optical morphology in the RTM calculations. This case yields the true DRE (DRE_{true}), which had a global mean value of +0.28 W/m². As expected, larger DRE values were obtained in global biomass-burning hotspots, namely, South America, Africa, and South and Southeast Asia. We note that DRE_{true} is true only in the context of our thought experiment because we calculated both b_{sca} and g using the simplified optical morphology. Figure 4b shows the difference between DRE_{true} and DRE calculated using the simplified optical morphology (Mie theory) in the RTM calculations and $k_{\text{OA,true}}$ ($\text{DRE}_{\text{simplified\&true}}$). Even though the two simulations use $k_{\text{OA,true}}$, $\text{DRE}_{\text{simplified\&true}}$ is substantially larger than DRE_{true} , with a global mean difference of +0.11 W/m² (40%), because the simplified optical morphology yields larger BC and OA absorption than the true optical morphology. On the other hand, when we use the simplified optical morphology both to retrieve k_{OA} and in the RTM calculations, the resulting DRE ($\text{DRE}_{\text{simplified\&simplified}}$) approaches DRE_{true} (global mean relative error < 4%). This indicates that when using a consistent simplified optical morphology both in the k_{OA} retrieval process and the RTM calculations, the underestimation of k_{OA} , thus OA absorption, is almost exactly counterbalanced by the overestimation of the total carbonaceous aerosol absorption. Simply put, the errors associated with consistently using overly simplified optical morphology are much smaller than those that result from measurement and modeling groups using different optical morphologies.

Due to the high computational cost, we performed detailed global RTM simulations for only a single morphology. To investigate the validity of our results for other morphologies, we performed simplified radiative transfer calculations using the formulation of Chen and Bond [2010] (see supporting information for details) to calculate the simple forcing efficiency (SFE). We explored a range of BC monomer size (10 nm–50 nm) and fraction of BC coated by OA (0.1–1). For each morphology in this 2-D space, we retrieved $k_{\text{OA,true}}$ and $k_{\text{OA,simplified}}$ as described in section 4. Similar to the detailed global simulations, we calculated SFE for the three cases: (1) true optical morphology and $k_{\text{OA,true}}$ (SFE_{true}), (2) simplified optical morphology and $k_{\text{OA,true}}$ ($\text{SFE}_{\text{simplified\&true}}$), and (3) simplified optical morphology and $k_{\text{OA,simplified}}$ ($\text{SFE}_{\text{simplified\&simplified}}$). As shown in Figure S2, the relative error in the mismatch case ($\text{SFE}_{\text{simplified\&true}}$) ranged between 35% and 75%, while the relative error in $\text{SFE}_{\text{simplified\&simplified}}$ was less than 3% regardless of the morphology, confirming the detailed global RTM results.

6. Discussion

To obtain accurate estimates of the DRE of carbonaceous aerosols containing light-absorbing OA, consistency in the assumed optical morphology between RTM calculations and the retrieval of OA light absorption properties from measurements is more important than the validity of the assumed optical morphology. This result indicates that Mie theory is an efficient transfer function to convert OA light absorption measurements to global DRE. On the other hand, using the true k_{OA} (retrieved using a realistic optical morphology) can lead to substantial errors in DRE calculated based on Mie theory, if the morphology of the particles substantially deviates from the simplified spherical representation. Therefore, as long as RTMs base their aerosol optical calculations on Mie theory, we recommend that the parametrizations of k_{OA} applied in these models be based on retrievals that also use Mie theory.

We stress that the call for consistency between measurement and RTM calculations is by no means a call for abandoning the investigation of the morphology of carbonaceous particles. This study focuses on the climate effect of OA light absorption, and the conclusions do not necessarily apply to other climate-relevant properties (e.g., cloud condensation nuclei activation) [Giordano *et al.*, 2015]. Furthermore, understanding the evolution of morphology upon atmospheric aging is of major importance. This work relies on the premise that there is no difference in morphologies observed during measurements and at climate-relevant atmospheric residence times. This premise would be challenged for near-source measurements if the morphology evolves

significantly upon aging in the atmosphere. However, while such evolution in morphology is expected for relatively pure BC aggregates (say in diesel emissions) as they mix with other species in the atmosphere, BC is usually already mixed with significant amounts of OA in biomass-burning emissions (the focus of this study). Therefore, we do not expect the optical morphology of biomass-burning particles to evolve significantly as a function of atmospheric age. Our findings do suggest that as these more complex life cycle changes are explored, it will be important for consistent treatments to be applied both for optical properties retrievals and for their representation in large-scale models.

Acknowledgments

Funding was provided by NSF grant AGS-1447056 and the U.S. EPA NCER through the STAR program (RD835438). The views, opinions, and/or findings contained in this paper are those of the authors and should not be construed as an official position of the funding agencies.

References

- Adachi, K., S. H. Chung, and P. R. Buseck (2010), Shapes of soot aerosol particles and implications for their effects on climate, *J. Geophys. Res.*, *115*, D15206, doi:10.1029/2009JD012868.
- Adler, G., A. A. Riziq, C. Erlick, and Y. Rudich (2010), Effect of intrinsic organic carbon on the optical properties of fresh diesel soot, *Proc. Natl. Acad. Sci. U.S.A.*, *107*(15), 6699–6704, doi:10.1073/pnas.0903311106.
- Anderson, G., S. Clough, F. Kneizys, J. Chetwynd, and E. Shettle (1986), AFGL atmospheric constituent profiles (0–120 km).
- Andreae, M. O., and A. Gelencser (2006), Black carbon or brown carbon? The nature of light-absorbing carbonaceous aerosols, *Atmos. Chem. Phys.*, *6*, 3131–3148.
- Bohren, C. F., and D. R. Huffman (1983), *Absorption and Scattering of Light by Small Particles*, Wiley, New York.
- Bond, T. C., and R. W. Bergstrom (2005), Light absorption by carbonaceous particles: An investigative review, *Aerosol Sci. Technol.*, *39*, 1–41, doi:10.1080/02786820500421521.
- Bond, T. C., D. G. Streets, K. F. Yarber, S. M. Nelson, J.-H. Woo, and Z. Klimont (2004), A technology-based global inventory of black and organic carbon emissions from combustion, *J. Geophys. Res.*, *109*, D14203, doi:10.1029/2003JD003697.
- Bond, T. C., G. Habib, and R. W. Bergstrom (2006), Limitations in the enhancement of visible light absorption due to mixing state, *J. Geophys. Res.*, *111*, D20211, doi:10.1029/2006JD007315.
- Cappa, C. D., et al. (2012), Radiative absorption enhancements due to the mixing state of atmospheric black carbon, *Science*, *337*(6098), 1078–1081, doi:10.1126/science.1223447.
- Chakrabarty, R. K., N. D. Beres, H. Moosmüller, S. China, C. Mazzoleni, M. K. Dubey, L. Liu, and M. I. Mishchenko (2014), Soot superaggregates from flaming wildfires and their direct radiative forcing, *Sci. Rep.*, *4*, 5508, doi:10.1038/srep05508.
- Chen, Y., and T. C. Bond (2010), Light absorption by organic carbon from wood combustion, *Atmos. Chem. Phys.*, *10*(4), 1773–1787.
- China, S., C. Mazzoleni, K. Gorkowski, A. C. Aiken, and M. K. Dubey (2013), Morphology and mixing state of individual freshly emitted wildfire carbonaceous particles, *Nat. Commun.*, *4*, 2122, doi:10.1038/ncomms3122.
- Di Lorenzo, R. A., and C. J. Young (2016), Size separation method for absorption characterization in brown carbon: Application to an aged biomass burning sample, *Geophys. Res. Lett.*, *43*, 458–465, doi:10.1002/2015GL066954.
- Feng, Y., V. Ramanathan, and V. R. Kotamarthi (2013), Brown carbon: A significant atmospheric absorber of solar radiation?, *Atmos. Chem. Phys.*, *13*(17), 8607–8621, doi:10.5194/acp-13-8607-2013.
- Fu, H., M. Zhang, W. Li, J. Chen, L. Wang, X. Quan, and W. Wang (2012), Morphology, composition and mixing state of individual carbonaceous aerosol in urban Shanghai, *Atmos. Chem. Phys.*, *12*, 693–707.
- Giordano, M., C. Espinoza, and A. Asa-Awuku (2015), Experimentally measured morphology of biomass burning aerosol and its impacts on CCN ability, *Atmos. Chem. Phys.*, *15*, 1807–1821.
- Jacobson, M. Z. (2012), Investigating cloud absorption effects: Global absorption properties of black carbon, tar balls, and soil dust in clouds and aerosols, *J. Geophys. Res.*, *117*, D06205, doi:10.1029/2011JD017218.
- Jacobson, M. Z. (2014), Effects of biomass burning on climate, accounting for heat and moisture fluxes, black and brown carbon, and cloud absorption effects, *J. Geophys. Res. Atmos.*, *119*, 8980–9002, doi:10.1002/2014JD021861.
- Kirchstetter, T. W., T. Novakov, and P. V. Hobbs (2004), Evidence that the spectral dependence of light absorption by aerosols is affected by organic carbon, *J. Geophys. Res.*, *109*, D21208, doi:10.1029/2004JD004999.
- Kordos, J. K., C. E. Scott, S. C. Farina, Y. H. Lee, C. L'Orange, J. Volckens, and J. R. Pierce (2015), Uncertainties in global aerosols and climate effects due to biofuel emissions, *Atmos. Chem. Phys.*, *15*, 8577–8596.
- Lack, D. A., and C. D. Cappa (2010), Impact of brown and clear carbon on light absorption enhancement, single scatter albedo and absorption wavelength dependence of black carbon, *Atmos. Chem. Phys.*, *10*(9), 4207–4220, doi:10.5194/acp-10-4207-2010.
- Lack, D. A., J. M. Langridge, R. Bahreini, C. D. Cappa, and A. M. Middlebrook (2012), Brown carbon and internal mixing in biomass burning particles, *Proc. Natl. Acad. Sci. U.S.A.*, *109*(37), 14,802–14,807.
- Lambe, A. T., et al. (2013), Relationship between oxidation level and optical properties of secondary organic aerosol, *Environ. Sci. Technol.*, *47*(12), 6349–6357, doi:10.1021/es401043j.
- Lin, G., J. E. Penner, M. G. Flanner, S. Sillman, L. Xu, and C. Zhu (2014), Radiative forcing of organic aerosol in the atmosphere and on snow: Effects of SOA and brown carbon, *J. Geophys. Res. Atmos.*, *119*, 7453–7476, doi:10.1002/2013JD021186.
- Liu, D., J. W. Taylor, D. E. Young, M. J. Flynn, H. Coe, and J. D. Allan (2015), The effect of complex black carbon microphysics on the determination of the optical properties of brown carbon, *Geophys. Res. Lett.*, *42*, 613–619, doi:10.1002/2014GL062443.
- Liu, S., et al. (2014), Aerosol single scattering albedo dependence on biomass combustion efficiency: Laboratory and field studies, *Geophys. Res. Lett.*, *41*, 742–748, doi:10.1002/2013GL058392.
- Liu, S., et al. (2015), Enhanced light absorption by mixed source black and brown carbon particles in UK winter, *Nat. Commun.*, *6*, 8435, doi:10.1038/ncomms9435.
- Mayer, B., and A. Kylling (2005), Technical note: The libRadtran software package for radiative transfer calculations – description and examples of use, *Atmos. Chem. Phys.*, *5*, 1855–1877.
- Mishchenko, M. I., L. Liu, and D. W. Mackowski (2013), T-matrix modeling of linear depolarization by morphologically complex soot and soot-containing aerosols, *J. Quant. Spectros. Radiat. Transfer*, *123*, 135–144.
- Moosmüller, H., and W. P. Arnott (2009), Particle optics in the Rayleigh regime, *J. Air Waste Manage. Assoc.*, *59*, 1028–1031.
- Petters, M. D., and S. M. Kreidenweis (2007), A single parameter representation of hygroscopic growth and cloud condensation nucleus activity, *Atmos. Chem. Phys.*, *7*, 1961–1971.

- Saleh, R., C. J. Hennigan, G. R. McMeeking, W. K. Chuang, E. S. Robinson, H. Coe, N. M. Donahue, and A. L. Robinson (2013), Absorptivity of brown carbon in fresh and photo-chemically aged biomass-burning emissions, *Atmos. Chem. Phys.*, *13*(15), 7683–7693, doi:10.5194/acp-13-7683-2013.
- Saleh, R., et al. (2014), Brownness of organics in aerosols from biomass burning linked to their black carbon content, *Nat. Geosci.*, doi:10.1038/ngeo2220.
- Saleh, R., M. Marks, J. Heo, P. J. Adams, N. M. Donahue, and A. L. Robinson (2015), Contribution of brown carbon and lensing to the direct radiative effect of carbonaceous aerosols from biomass and biofuel burning emissions, *J. Geophys. Res. Atmos.*, *120*, 10,285–10,296, doi:10.1002/2015JD023697.
- Schnaiter, M. (2005), Absorption amplification of black carbon internally mixed with secondary organic aerosol, *J. Geophys. Res.*, *110*, D19204, doi:10.1029/2005JD006046.
- Schwarz, J. P., et al. (2008), Measurement of the mixing state, mass, and optical size of individual black carbon particles in urban and biomass burning emissions, *Geophys. Res. Lett.*, *35*, L13810, doi:10.1029/2008GL033968.
- Sorensen, C. M. (2001), Light scattering by fractal aggregates: A review, *Aerosol Sci. Technol.*, *35*, 648–687.
- Stamnes, K., S. C. Tsay, W. Wiscombe, and I. Laszlo (2000), DISORT, a General-Purpose Fortran Program for Discrete-Ordinate-Method Radiative Transfer in Scattering and Emitting Layered Media: Documentation of Methodology.
- Wang, X., C. L. Heald, D. A. Ridley, J. P. Schwarz, J. R. Spackman, A. E. Perring, H. Coe, D. Liu, and A. D. Clarke (2014), Exploiting simultaneous observational constraints on mass and absorption to estimate the global direct radiative forcing of black carbon and brown carbon, *Atmos. Chem. Phys. Discuss.*, *14*(11), 17,527–17,583, doi:10.5194/acpd-14-17527-2014.
- Wu, Y., T. Cheng, L. Zheng, and H. Chen (2016), Optical properties of the semi-external mixture composed of sulfate particle and different quantities of soot aggregates, *J. Quant. Spectros. Radiat. Transfer*, *179*, 139–148.
- Yurkin, M. A., and A. G. Hoekstra (2011), The discrete-dipole-approximation code ADDA: Capabilities and known limitations, *J. Quant. Spectros. Radiat. Transfer*, *112*, 2234–2247.
- Zhang, R., A. F. Khalizov, J. Pagels, D. Zhang, H. Xue, and P. H. McMurry (2008), Variability in morphology, hygroscopicity, and optical properties of soot aerosols during atmospheric processing, *Proc. Natl. Acad. Sci. U.S.A.*, *105*(30), 10,291–10,296, doi:10.1073/pnas.0804860105.
- Zhu, J., P. A. Crozier, and J. R. Anderson (2013), Characterization of light-absorbing carbon particles at three altitudes in East Asian outflow by transmission electron microscopy, *Atmos. Chem. Phys.*, *13*, 6359–6371.